Modelling Multi-connectivity in 5G NR Systems with Mixed Unicast and Multicast Traffic

Vitalii Beschastnyi[1(✉)], Daria Ostrikova[1], Sergey Melnikov[1], and Yuliya Gaidamaka[1,2]

[1] Peoples' Friendship University of Russia (RUDN University), 6 Miklukho-Maklaya St, Moscow 117198, Russian Federation
{beschastnyy-va,ostrikova-dyu}@rudn.ru, melnikov@linfotech.ru
[2] Federal Research Center "Computer Science and Control" of the Russian Academy of Sciences (FRC CSC RAS), 44-2 Vavilov St, Moscow 119333, Russian Federation
gaydamaka-yuv@rudn.ru

Abstract. 3GPP New Radio (NR) radio access technology operating in millimeter wave (mmWave) frequency band is considered as key enabler for Fifth-generation (5G) mobile system. Despite the enormous available bandwidth potential, mmWave signal transmissions suffer from fundamental technical challenges like severe path loss, sensitivity to blockage, directivity, and narrow beamwidth, due to its short wavelengths. To address the problem of quality degradation due to the line-of-sight (LoS) blockage by various objects in the channel, 3GPP is currently working on multi-connectivity (MC) mechanisms that allow a user to remain connected to several mmWave access points simultaneously as well as switch between them in case its active connection drops. In this paper, exploiting the methods of stochastic geometry and queuing theory we propose a model of 5G NR base station (BS) serving a mixture of unicast and multicast traffic. MC techniques is proposed to be used for cell-edge users. The proposed model is validated against computer simulations in terms of session drop probabilities and system resource utilization metrics. Our findings are illustrated with a numerical example.

Keywords: 5G NR · mmWave · Multi-connectivity · simulation

1 Introduction

Every year, user needs and the number of device connections are increasing. According to the Cisco statistics [1], mobile video traffic has been believed to

The publication has been prepared with the support of the "RUDN University Program 5–100" (V.A. Beschastnyi, original draft preparation; D.Yu. Ostrikova, visualization and validation). The reported study was funded by RFBR, projects Nos. 18-07-00156 (Yu.V. Gaidamaka, conceptualization and methodology) and 18-07-00576 (Yu.V. Gaidamaka, supervision and project administration).

V. M. Vishnevskiy et al. (Eds.): DCCN 2020, LNCS 12563, pp. 52–63, 2020.
https://doi.org/10.1007/978-3-030-66471-8_5

increase by 50 percent annually. Due to the growing popularity of multifunctional multimedia applications and services, wireless mobile networks must constantly evolve, offering higher data rates, as well as reducing data transfer delays and increasing energy efficiency, which leads to an increase in the quality of service for end users. 3GPP New Radio (NR) radio access technology standardized by 3rd Generation Partnership Project (3GPP) [2] is expected to play a key role in 5G systems. NR systems promise multi-gigabit rates together with reduced latency at the air interface compared to 4G Networks. Despite the enormous available bandwidth potential, mmWave signal transmissions suffer from fundamental technical challenges like severe path loss, sensitivity to blockage, directivity, and narrow beamwidth, due to its short wavelengths. To effectively support system design and deployment, accurate channel modeling comprising several 5G technologies and scenarios is essential [3,4]. Though mmWave frequency band offers huge amount of available resources, the lack of PTM capabilities may imply a future limitation of 5G networks, leading to inefficient service provisioning and utilization of the network and spectrum resources [5–7].

In indoor scenarios 5G NR systems mostly suffer from obstacles such as humans and vehicles, which generally tend to be mobile and are often termed "blockers" [8]. For the sake of block error probability mitigation at the air interface a user equipment (UE) experiencing such type of blockage may lower its modulation and coding scheme (MCS) that depends on propagation environment and the distance to NR base station (BS), or enter outage conditions in case further lowering of MCS is impossible [9]. Multi-connectivity operation recently proposed by 3GPP is aimed at solving the problem of outage conditions by maintaining several simultaneously active links for adjacent NR BSs so that the connection is redirected between them in case of blockage [10,11]. However, when lowering MCS, additional physical resources are utilized to support the required rate at the air interface. Once the required amount of resource in not available, a session should either reduce its rate, or it should be dropped [3].

In [12] authors introduce a joint scheduling framework based on dynamic MC to satisfy the different requirements of enhanced mobile broadband (eMBB) and ultra-reliability low-latency communication (URLLC) traffics in 5G. The framework aims to optimize multiple traffics in independent link dynamically. BSs will form MC clusters, which vary with network characteristics to accomplish high rate. Maximum capacity of eMBB traffic is achieved while the latency of the uRLLC traffics is guaranteed. The authors of [13] characterize the outage probability and spectral efficiency associated with different degrees of MC in a typical 5G urban scenario, where the line-of-sight propagation path can be blocked by buildings as well as humans. These results demonstrate that the degrees of MC of up to 4 offer higher relative gains.

In this paper, we consider a 5G NR BS deployment serving mixture of unicast and multicast sessions. MC techniques is proposed to be used for cell-edge users. First, by means of stochastic geometry we derive the amount of required resource in terms of average values that will further simplify our computations. Then, we present our simulation approach and finally validate our model against

computer simulations. Our findings showed the advantages of multicast sessions over unicast ones in terms of reliability and resource consumption.

The remainder is organized as follows. First, our system model of NR BS operation under unicast and multicast traffic load introduced in Section 2. The simulation approach is offered in Sect. 3. Numerical results illustrating the resource occupation effect of multicast sessions are presented in Section 4. Conclusions are drawn in the last section.

2 System Model

This section provides an overview of the considered scenario with 5G NR Base Station that serves unicast (point-to-point, PTP) and multicast (point-to-multipoint, PTM) sessions[14]. As we assume only rather small mobile obstacles in our model, the BS has circularly-shaped coverage area of radius d^E_{LoS}. We assume random distribution of users that follows Poisson Point Process (PPP) with density parameter ρ. The coverage area radius can be evaluated using the mmWave propagation model mentioned below together with MCSs what gives us the SNR threshold at which the session can be no longer served at current BS. The mapping between CQIs and spectral efficiency for 3GPP NR systems is given in Table 1 where LoS ad n nLoS ranges are estimated for the default system paramenters presented in Sect. 4. This approach follows [3], where authors compute mean demand for the model without multiconnectivity feature.

Table 1. CQI, MCS, and distance mapping.

CQI, i	MCS	$E(i)$	SNR, [dB]	LoS range, [m]	nLoS range [m]
1	QPSK, 78/1024	0,15237	–9,478	758–1033	146–199
2	QPSK, 120/1024	0,2344	–6,658	572–758	111–146
3	QPSK, 193/1024	0,377	–4,098	445–572	86–111
4	QPSK, 308/1024	0,6016	–1,798	350–445	68–86
5	QPSK, 449/1024	0,877	0,399	280–350	54–68
6	QPSK, 602/1024	1,1758	2,424	223–280	43–54
7	16QAM, 378/1024	1,4766	4,489	182–223	35–43
8	16QAM, 490/1024	1,9141	6,367	145–182	28–35
9	16QAM, 616/1024	2,4063	8,456	119–145	23–28
10	16QAM, 466/1024	2,7305	10,266	96–119	18–23
11	16QAM, 567/1024	3,3223	12,218	78–96	15–18
12	16QAM, 666/1024	3,9023	14,122	64–8	12–15
13	16QAM, 772/1024	4,5234	15,849	52–64	10–12
14	16QAM, 873/1024	5,1152	17,786	42–64	8–10
15	16QAM, 948/1024	5,5547	19,809	0–42	0–8

When establishing a user session, BS allocates the amount of physical resource that is generally a random variable and depends on propagation model and the distance from UE to the serving BS. According to [15,16], the mmWave linear path loss L in dBs for UEs in LoS and nLoS conditions is given by:

$$L(x) = \begin{cases} 32.4 + 21\log(x) + 20\log f_c, \text{non-blocked}, \\ 47.4 + 21\log(x) + 20\log f_c, \text{blocked}, \end{cases}$$

where f_c is operational frequency measured in GHz, and x is the distance between BS and UE. These expressions allow us deriving maximum distances d^E_{nLoS} and d^E_{LoS} at which a UE is able to start a session in blocked and non-blocked conditions correspondingly. This can be done by taking the lowest SNR defined by MCS as the value of L threshold [9,15].

In our model the coverage area is divided into two sectors: "inner sector (zone)" with radius $R_I = d^E_{nLoS}$; and the "outer sector (zone)" with width $R_O = R_C - R_I$, where R_O is restricted by the radius of the coverage area R_C. This division allows us for improving resource demand estimation as demands of sessions from inner zone that are always served at the same BS considerably different from sessions from outer zone that are subject of MC mechanism.

Then, to define the resource demands $b^{(n)LoS}_{I/O}$ that depend on both UE location (inner or outer zone) and LoS conditions we use approximations of spectral efficiency for each of the four propagation scenarios. The approximations are performed as the following: first, using the conventional MCS we define the longest possible distances x_i for each given i-CQI in LoS and nLoS conditions (1); then we calculate the coverage area for the CQIs as $\Omega_i = \pi(x_i^2 - x_{i-1}^2)$ for i-CQI, $x_0 = 0$; finally, we derive the average resource demand for each of the scenarios (2).

$$x_i = \begin{cases} \left(\frac{P_A G_A G_U}{S_i N_0 W \left(10^{2\log_{10} f_c + 3.24}\right)} \right)^{\frac{1}{\gamma}}, \text{non-blocked}, \\ \left(\frac{P_A G_A G_U}{S_i N_0 W \left(10^{2\log_{10} f_c + 4.74}\right)} \right)^{\frac{1}{\gamma}}, \text{blocked}, \end{cases} \tag{1}$$

where P_A is the NR BS transmit power, S_i is the worst possible SNR given by MCS for i-CQI, G_A and G_U are the antenna array gains at the NR BS and the UE ends, respectively, N_0 is the power spectral density of noise, W is the given bandwidth, γ – path loss exponent.

$$b^{(n)LoS} = \begin{cases} \left\lceil v \cdot \left(s_A \cdot \sum\limits_{i: 0 < x_i \le R_I} \frac{\Omega_i^{(n)LoS} \cdot E_i}{R_I} \right)^{-1} \right\rceil, \text{inner zone}, \\ \left\lceil v \cdot \left(s_A \cdot \sum\limits_{i: R_I < x_i \le R_C} \frac{\Omega_i^{(n)LoS} \cdot E_i}{R_C} \right)^{-1} \right\rceil, \text{outer zone}, \end{cases} \tag{2}$$

where s_A is the physical resource block (PRB) measured in MHz, E_i is the spectral efficiency corresponding to i-CQI, v is the required service data rate.

Mobile obstacles may appear on LoS towards the BS and thus reduce the SNR of the established connection. In this paper we consider the typical type of blockers for indoor scenarios which is humans with their blockage radius r_B approximating the width of human body. We model blockers' movement with two exponentially distributed random variables with parameters θ_{LoS} and θ_{nLoS} that correspond to the time intervals when a blocker is passing the LoS and periods between two consecutive blockage events [3]. It should be noted that the θ_{LoS} and θ_{nLoS} intensities generally depend on density of users and their behaviour, i.e. their velocity and mobility model. It means that in case of dense networks, system performance may be severely compromised not only by the number of active devices, but also the increased LoS blocking probability.

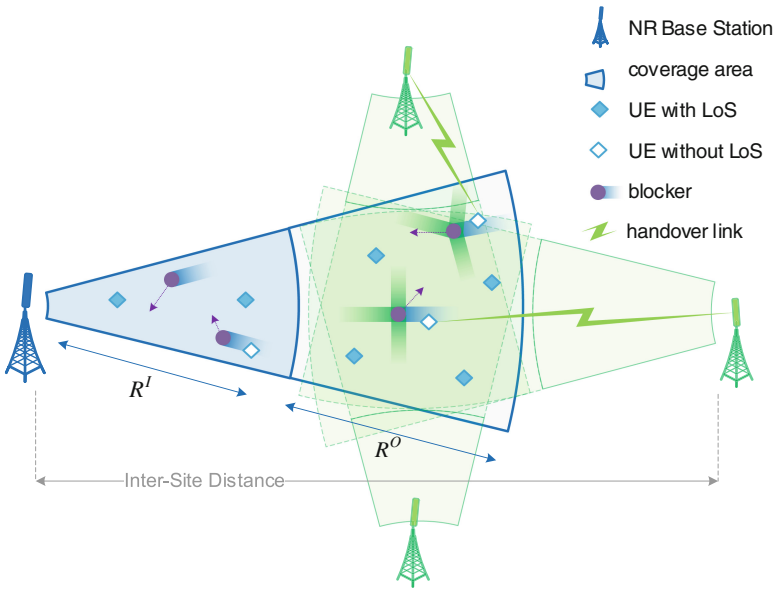

Fig. 1. Communication scenario.

Figure 1 illustrates the communication scenario considered in our paper. We observe the resource allocation process at a single NR BS. We suppose there are no interfering beams that could worsen channel quality. Each blocker has its own radio shadow area with length $d_B = \frac{d(h_B - h_U)}{(h_A - h_U)} + r_B$ [3]. Inside inner zone UE has only one active link with the target NR BS, resources are allocated even if UE in the radio shadow area. As the MCS does not support connection in nLoS conditions whenever UE at the distance $d > R^I$, multiple links are maintained towards the target and nearby BSs; once it gets into the shadow, user session is handed over to the BS with the greatest SNR at the moment.

As we assume that NR BS maintains constant bitrate for an established session, in our model session is only dropped when its new demand is more than remaining resource. Session requires additional resource in the following cases: (i) new session is initiated; (ii) LoS towards UE is blocked in inner zone; (iii) ongoing session is handed over back to original NR BS.

We also assume that there is no prioritization among traffic types. Whenever a session is attempting for establishment, NR BS allocates unoccupied resource without any reservation mechanisms [17].

3 Simulation Approach

In this section we present the system-level tool that we used to validate the above-mentioned model. As we have limited system capacity in terms of resource, this guarantees accessibility of steady-state conditions [18] that are detected using exponentially-weighted moving average technique with smoothing parameter set to 0.05.

The simulation tool utilizes an event-driven engine that allows for processing predefined set of events [19,20], such as session establishment and aborting, blockages, handover, resource management, etc. This approach provides both much flexibility and powerful capabilities for statistic data collection. High-level algorithm of the simulation is described as UML activity diagram presented in Fig. 2.

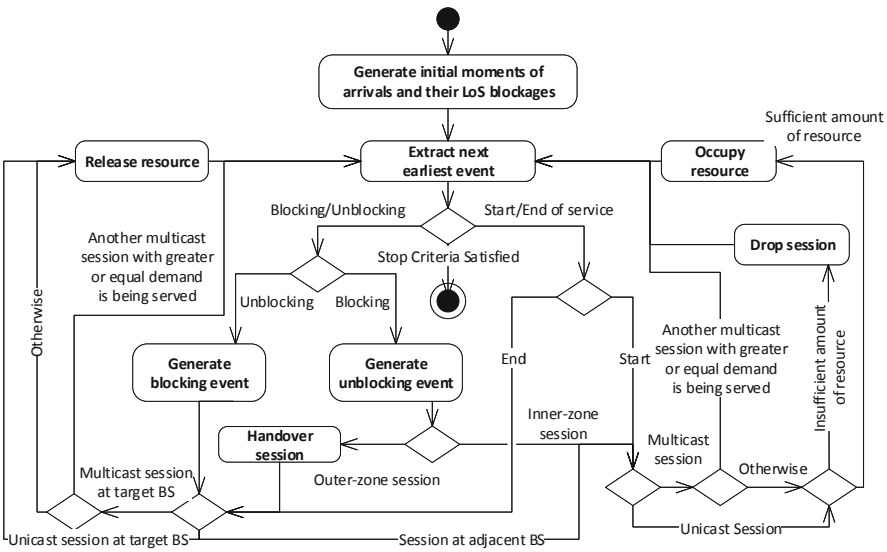

Fig. 2. Simulation algorithm.

Data is collected during the steady-state period only providing better accuracy compared to analytical results. In what follows, we demonstrate only point estimates of the metrics of interest.

4 Numerical Assessment

In this paper, we analyze NR BS resource allocation process needed for establishing and maintaining unicast and multicast [21] sessions composing mixed traffic load. Our metrics of interest are unicast and multicast session drop probabilities and mean NR BS resource utilization which are the key indicators of system reliability. The input system parameters [22] are given in Table 2.

Table 2. Input data

Notation	Description	Values
P_A	Transmit power	0.2 W
G_A	BS antenna array gain	2.58 dBi
G_U	UE antenna array gain	2.58 dBi
f_c	Operational frequency	28 GHz
W	Bandwidth	1 GHz
s_A	Service unit	1.44 MHz
N_0	Density of noise	–84 dBi
γ	Path loss exponent	2.1
r_B	Blocker radius	0.4 m
h_B	Blocker height	1.7 m
h_U	UE height	1.5 m
h_A	NR BS height	4 m
R_O	Outer zone radius	200 m
R_I	Inner zone radius	200 m
d_{ISD}	Inter site distance	600 m
v	Service data rate	64–5120 kbps
θ_{nLoS}^{-1}	Mean blockage time	2.94 s
λ^{-1}	Session mean inter-arrival time	200–2000 s
μ^{-1}	Mean service time	1–3600 s

The traffic profile (Table 3) complies with the global traffic forecast for 2025 [23], while service characteristics provided in [24]. We consider six types of services: streaming video [25], audio, file sharing, social networking, Web, and Machine-to-Machine [26] traffic. Data is transmitted by unicast sessions for all the services, but video can be also streamed via multicast sessions to reduce the amount of utilized resource.

Table 3. Service characteristics.

Service	Data rate, [kbps]	Duration, [s]	Share, [%]
Video	5120	3600	76
Audio	64	90	1
File sharing	1024	2	3
Social networking	384	8	8
Web browsing	500	3	2
M2M	200	1	10

In Fig. 3 and Fig. 4 we present session drop probabilities for different density values. One may observe extremely rapid degradation of unicast video service compared to other services. This can be explained by the huge resource demand of video traffic coupled with long-lasting service delivery time. It is much easier for services with smaller demands to fit into the remainder of the resources in case of high traffic load at NR BS.

Figure 4 shows that in case of handover sessions the gap between video and other types of services in terms of session continuity becomes even greater.

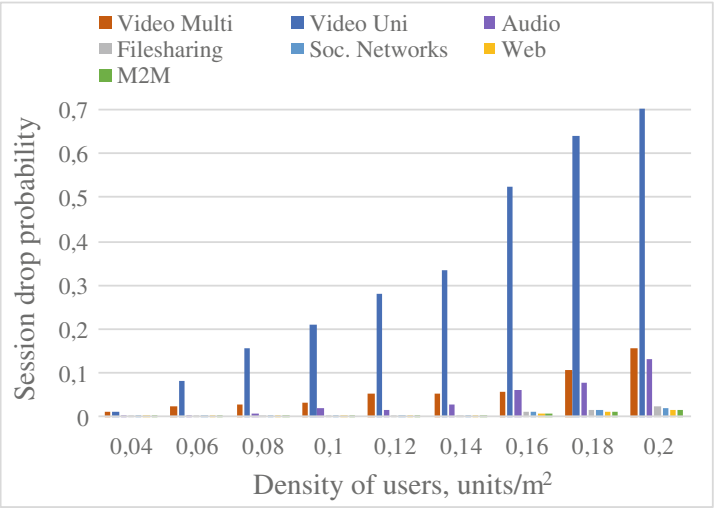

Fig. 3. Session drop probabilities.

In Fig. 5 we demonstrate resource distribution among the above-mentioned services. Along with the network densification the share of resource occupied by video traffic declines, ceding it to the more light-weight and short-time services.

We also present numerical results for session drop probabilities (Fig. 6) as function of inter-site distance for different ratio between unicast and multicast

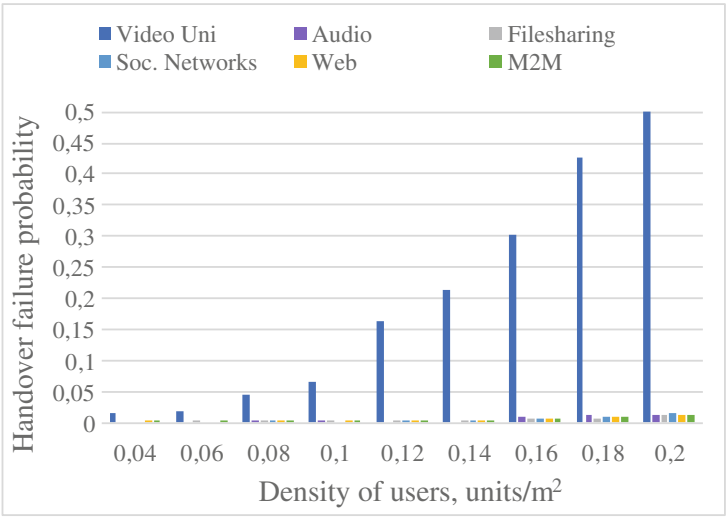

Fig. 4. Handover failure probabilities.

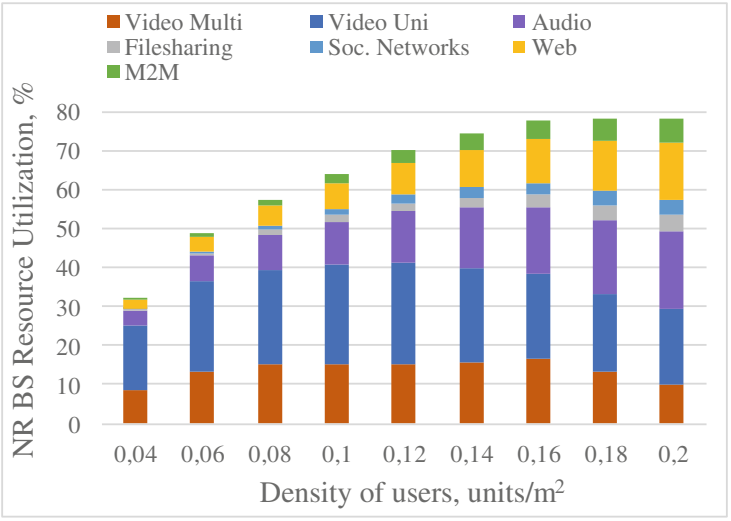

Fig. 5. Resource utilization.

traffic shares. As may be observed, the trend of unicast numerical superiority over multicast in drop probabilities is mainly kept within all the variety of traffic shares. However, when the number of multicast sessions becomes insufficient to continuously occupy allocated amount of resource, the multicast session drop probabilities start to outnumber unicast ones.

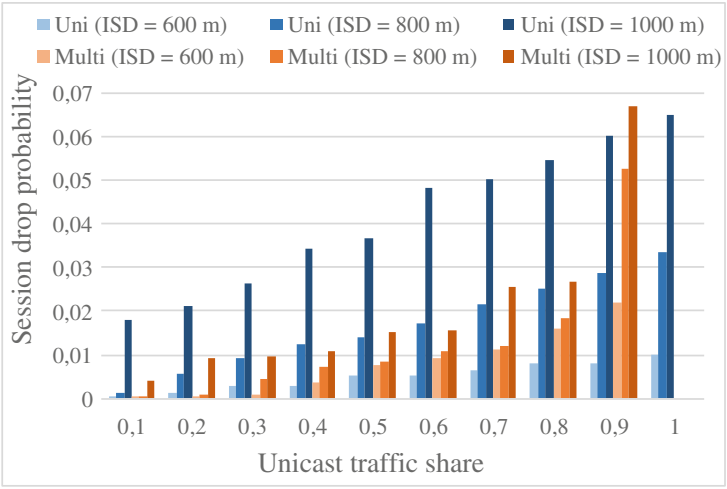

Fig. 6. Session drop probabilities as function of ISD.

By setting a threshold at some maximum allowed value of drop probability, it is possible to estimate the longest possible distance between adjacent NR BSs. Such approach allows for optimization of NR BS deployment minimizing the number of BSs to provide acceptable coverage within a given area. This may significantly reduce capital and operations expenses of network operator, but in this case one should give thorough consideration to the network scalability.

Our findings show that multicast sessions offer more reliability compared to unicast communications providing four-times less drop rates while occupying less amount of resource. This can be explained by the concept of resource occupation while organizing a multicast session. Once amount of resource is allocated to a multicast session, all the successive multicast sessions providing the access to the same content will keep on capturing this resource until the last session comes to its end.

5 Conclusion

In this paper, we considered the radio frequency resource allocation by a 5G NR BS with multi-connectivity mechanism that allows for reducing density of BS deployment. By means of the developed simulation tool we provided the numerical analysis of 5G NR BS deployment serving mixture of unicast and multicast sessions. Our findings revealed the advantages of multicast sessions over unicast ones in terms of reliability and resource consumption.

Our future work is to study fair radio resources distribution policies between unicast and multicast multimedia services in next-generation mobile networks that allow to protect disadvantaged types of services to fulfil QoE requirements.

References

1. Cisco Visual Networking Index: Forecast and Methodology, 2017–2022 White Paper (2019). https://www.cisco.com/c/en/us/solutions/collateral/serviceprovider/visual-networking-index-vni/white-paper-c11-741490.html
2. IEEE Standard: 802.11ad-2012: Enhancements for Very High Throughput in the 60 GHz Band. https://ieeexplore.ieee.org/document/6392842/
3. Kovalchukov, R., et al.: Improved session continuity in 5G NR with joint use of multi-connectivity and guard bandwidth. In: 2018 IEEE Global Communications Conference (GLOBECOM), pp. 1–7 (2018)
4. Begishev, V., Samuylov, A., Moltchanov, D., Machnev, E., Koucheryavy, Y., Samouylov, K.: Connectivity properties of vehicles in street deployment of 3GPP NR systems. In: 2018 IEEE Globecom Workshops, GC Wkshps 2018 - Proceedings, art.no. 8644102 (2019)
5. Garro, E., Fuentes, M., Gomez-Barquero, D., Carcel, J.L.: 5G mixed mode: an innovative point-to-multipoint solution for new radio. In: 2019 IEEE International Symposium on Broadband Multimedia Systems and Broadcasting (BMSB), pp. 1–5 (2020)
6. Wang, J., Hongbo, X., Zhu, B., Fan, L., Zhou, A.: Hybrid beamforming design for mmWave joint unicast and multicast transmission. IEEE Commun. Lett. **22**(10), 2012–2015 (2018)
7. Säily, M., Barjau, C., Navrátil, D., Prasad, A., Gómez-Barquero, D., Tesema, F.B.: 5G radio access networks: enabling efficient point-to-multipoint transmissions. IEEE Vehicular Technol. Mag. **14**(4), 29–37 (2019)
8. Samuylov, A.: Characterizing resource allocation trade-offs in 5G NR serving multicast and unicast traffic. IEEE Trans. Wirel. Commun. **19**(5), 3421–3434 (2020)
9. 3GPP, "NR: Physical channels and modulation (Release 15)", 3GPP TR 38.211 (2017)
10. 3GPP, "NR: Multi-connectivity; Overall description (Release 15)", 3GPP TS 37.34 V15.2.0 (2018)
11. Petrov, V., et al.: Dynamic multi-connectivity performance in ultra-dense urban mmWave deployments. IEEE J. Selected Areas Commun. **35**(9), 2038–2055 (2017)
12. Zhang, K., Zhang, J., Tao, X.: Dynamic multiconnectivity based joint scheduling of eMBB and uRLLC in 5G networks. IEEE Syst. J., 1–11 (2020)
13. Gapeyenko, M., Petrov, V., Riza, M., Andreev, S., Himayat, N., Koucheryavy, Y.: On the degree of multi-connectivity in 5G millimeter-wave cellular urban deployments. IEEE Trans. Vehicular Technol. **6**(2), 1973–1978 (2018)
14. Feng, W., Li, Y., Niu, Y., Su, L., Jin, D.: Multicast spatial reuse scheduling over millimeter-wave networks. In: Wireless Communications and Mobile Computing Conference (IWCMC), pp. 317–322. IEEE (2017)
15. Polese, M., Zorzi, M.: Impact of channel models on the end-to-end performance of Mmwave cellular networks. In: IEEE 19th International Workshop on Signal Processing Advances in Wireless Communications (SPAWC), pp. 1–5 (2018)
16. Biason, A., Zorzi, M.: Multicast via Point to multipoint transmissions in directional 5G mmWave communications. IEEE Commun. Mag. **57**(2), 88–94 (2019)
17. Moltchanov, D., et al.: Improving session continuity with bandwidth reservation in mmwave communications. IEEE Wirel. Commun. Lett. **8**(1), 05–108 (2019)
18. Naumov, V., Samouylov, K.: Analysis of multi-resource loss system with state-dependent arrival and service rates. Prob. Eng. Inf. Sci. **31**(4), 413–419 (2017)

19. Mezzavilla, M., et al.: End-to-end simulation of 5G mmWave networks. IEEE Comm. Surv. Tutor. **20**(3), 2237–2263 (2018)
20. Samouylov, K., Naumov, V., Sopin, E., Gudkova, I., Shorgin, S.: Sojourn time analysis for processor sharing loss system with unreliable server. In: Wittevrongel, S., Phung-Duc, T. (eds.) ASMTA 2016. LNCS, vol. 9845, pp. 284–297. Springer, Cham (2016). https://doi.org/10.1007/978-3-319-43904-4_20
21. Vikhrova, O., Pizzi, S., Sinitsyn, I., Molinaro, A., Iera, A., Samuylov, K., Araniti, G.: An analytic approach for resource allocation of IoT multicast traffic. In: Proceedings of the International Symposium on Mobile Ad Hoc Networking and Computing (MobiHoc), pp. 25–30 (2019)
22. Samuylov, A., Moltchanov, D., Krupko, A., Kovalchukov, R., Moskaleva, F., Gaidamaka, Yu.: Performance analysis of mixture of unicast and multicast sessions in 5G NR systems. In: 10th International Congress on Ultra Modern Telecommunications and Control Systems and Workshops (ICUMT - 2018), Russia, Moscow (2018)
23. Ericsson Mobility Report (2020). https://www.ericsson.com/49da93/assets/local/mobility-report/documents/2020/june2020-ericsson-mobility-report.pdf
24. Khatibi, S., Correia, L.M.: Modelling virtual radio resource management in full heterogeneous networks. EURASIP J. Wirel. Commun. Netw. **2017**(1), 1–17 (2017). https://doi.org/10.1186/s13638-017-0858-7
25. Borodakiy, V.Y., Samouylov, K.E., Gudkova, I.A., Markova, E.V.: Analyzing mean bit rate of multicast video conference in LTE network with adaptive radio admission control scheme. J. Math. Sci. **218**(3), 257–268 (2016)
26. Gudkova, I., et al.: Analyzing impacts of coexistence between M2M and H2H communication on 3GPP LTE system. In: Mellouk, A., Fowler, S., Hoceini, S., Daachi, B. (eds.) WWIC 2014. LNCS, vol. 8458, pp. 162–174. Springer, Cham (2014). https://doi.org/10.1007/978-3-319-13174-0_13